Impact of Electric Vehicle Charging Control on the Frequency Response: Study of the GB System

Francisco Sánchez and Francisco Gonzalez-Longatt
Centre for Renewable Energy Systems Technology
(CREST)
Loughborough University
Loughborough, United Kingdom
F.Sanchez@lboro.ac.uk, fglongatt@fglongatt.org

José Luis Rueda and Peter Palensky
Department of Electrical Sustainable Energy
Delft University of Technology
(TU Delft)
Delft, Netherlands
J.L.RuedaTorres@tudelft.nl, P.Palensky@tudelft.nl

***Abstract*—The growth of vehicle electrification is driven by the desire to reduce environmental pollution, and it is fueled by advancements in battery technology. If left unmanaged, electric vehicle (EV) charging will increase peak demand and put a strain on the electricity networks. However, if properly managed, EVs can provide useful services to the power system operator such as fast active-power injection which serves to improve the system frequency response (SFR) after a disturbance. The objective of this paper is to assess the impact that clusters of EVs, connected to frequency-responsive charging stations, have on the provision of SFR after a loss of generation event. The assessment considers EV charging demand in Great Britain (GB) for the year 2025 considering three different daily charging patterns. A generic model for the EV clusters is developed which includes the effects of measurement delays and control charger time response. The model and scenarios are integrated into a single-area model representative of the GB power system and the minimum expected values for the system's inertia in the year 2025 are used. The results obtained highlight the benefits on the SFR of utilizing EVs as a dynamic energy storage system for different types of charging and the impact of the measurement delay on the dynamics of the response.**

***Index Terms*—Electric Vehicles, System Frequency Response, EV Load Estimation.**

I. Introduction

The number of electric vehicles (EVs) worldwide has been growing at an increasing rate since 2010, and it surpassed two million in 2016 [1]. It is expected the EV stock worldwide will reach between 40 and 70 million by the year 2025 [1]. The uptake of EVs brings several environmental benefits such as the improvement of air quality and the potential reduction in CO_2 emissions and it is mainly fueled by massive improvements in battery technology [2]. However, the massive uptake of EVs presents a challenge for the power system operation. For instance, if the charging of the vehicles is left unmanaged, an additional demand of between 4 to 8 GW could arise at peak times in the Great Britain (GB) power system [3].

The possibility of managing the charging pattern of the EVs to provide ancillary services such as frequency containment (FC), load balance and the spinning reserve has been explored in [4]. The FC refers to the ability to stabilize the frequency of the system following a disturbance, and this is extremely important given the rapidly of non-synchronically connected renewable generation which do not contribute to the system rotational inertia. The figure of the EV aggregator is an entity that acts as a coordinator between the EV owners and the system operators, offering the opportunities for new services.

The authors in [5] use the aggregation concept of a small group of EVs in order to provide frequency control via unidirectional charging. A frequency-droop controller for EV charger is designed for primary frequency response in [6], but the effect of measurement delays is not included. In [7], the EVs are modelled as a single Virtual Energy Storage System (VESS) in order to provide frequency regulation and to assist in the integration of intermittent wind energy, however, a single power-frequency characteristic is assigned to all the EVs in the VESS. Since EVs are available to provide frequency services only when they are connected to the charging station, an accurate estimate of the amount of EVs that will be connected at any given the time of day is of utmost importance for aggregator entities, distribution system operators (DSO) and transmission system operators (TSO).

The objective of this paper is to assess the impact of frequency-sensible EV chargers in the provision of system frequency services. Clusters of EVs with different charging patterns are used to assess the system frequency response (SFR) of a simplified version of the GB power system by the year 2025.

This paper unfolds three contributions: 1) the aggregated daily demand (30-min resolution) from EV charging is estimated for a typical day in the year 2025 considering the stochasticity of the travel behaviour and for different charging patterns in GB (Section IV). 2) a frequency response model of an EV cluster is developed considering the characteristics of the EV charging stations (Sections II and III). 3) simulation results are used to define the impact of (i) the type of charging, (ii) the charger time constant, (iii) the measurement delay, (iv) the time of charging and (v) the EV penetration on the frequency of the system following a disturbance (Section VI).

The paper is structured as follows: Section II presents the modelling details of the SFR of the power system and the cluster of aggregated EVs. Section III defines the model of frequency-responsive charger stations based on the location of the charging. An estimation of the charging demand for GB in

the year 2025 depending on the charging patterns of the EV user is presented in Section IV. Sections V and VI present the simulation scenarios and the numerical results, respectively. Finally, Section VII presents the conclusions and future research directions.

II. System Frequency Response Modelling considering EV Clusters

The classical SFR model of an isolated power system [8] has been enhanced in order to include the frequency response of the aggregated effect of a cluster of EVs (see Fig 1). In this paper, the main concern is the provision of fast-active power injection from EVs therefore the slower effects of secondary control loops and interchange of power between areas are neglected.

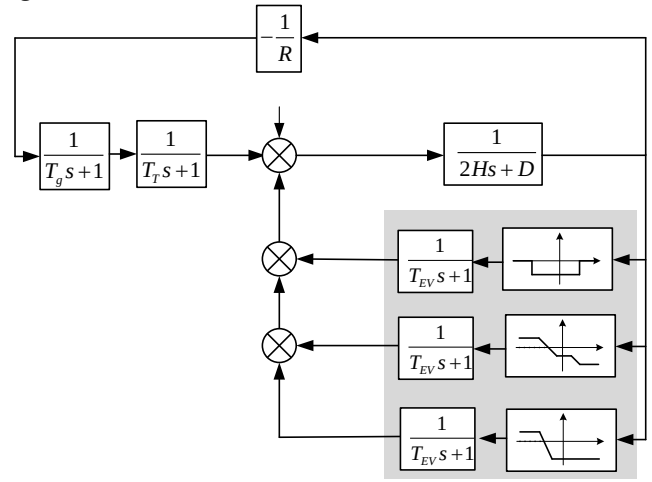

Fig. 1. SFR model of a single-area power system model considering the frequency response of a cluster of EVs.

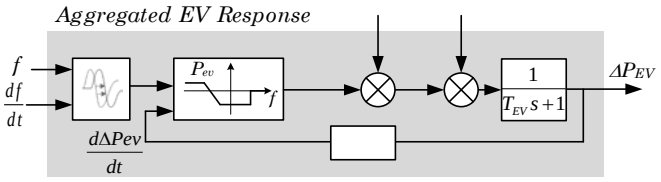

Fig. 2. SFR model of an aggregated cluster of EV cluster including the dynamic of the EV charger.

The dynamic of the system frequency of the SFR model shown in Fig. 1 is described by:

$$\frac{d\Delta f}{dt} = \frac{\Delta P_G + \Delta P_{EV} - \Delta P_L - D\Delta f}{2H} \quad (1)$$

The first order differential equation (1) describes the rate of change of the system's frequency (*ROCOF* = $d\Delta f/dt$) when a disturbance in demand (ΔP_L) or generation (ΔP_G) suddenly arises. The rotational inertia constant (H), represents the normalized kinetic energy stored in the rotating element of the generating machines at synchronous speed (ω_s) and the damping parameter (D), models the variation in demand with respect to a frequency change (Δf). The speed-droop parameter (R), models the change in the energy input to the generator's prime mover in response to frequency changes in the system. The variable ΔP_{EV} represents the change in the power injected into the system by the EVs contributing to frequency support.

A. Power-Frequency (P-f) Model of EV Charger

The SFR model of the aggregated cluster of EVs is based in a frequency-sensible curve based on active-power frequency (Fig. 2). The model of the cluster of EVs consists of a measurement delay block, a power-frequency (*P-f*) control block and a charger delay block. The inputs to the block are the system's frequency (*f*) and its rate of change (*df/dt*), scaling parameters $P_{EV,Base}$ and $P_{EV,Ref}$ which are related to the EV demand at each time period (30-min) during the day and to the type of control provided by the charging station respectively. The block's output is the change in electric power demand of the EVs, ΔP_{EV}. A positive value of ΔP_{EV} represents a decrease in demand or an increase in active power. The components of the EV cluster block are (i) *Measurement and charger delay blocks*: These blocks model the delay in the measurement and communication processes as well as the delay imposed by the EV charger, T_{EV} [7]. (ii) *EV P-f Control block*: This block outputs the power set point for the EV cluster based on the system frequency and according to predefined ramps and dead bands which depend on the type of charging station as explained in Section III. The block also controls the power set point based on the ROCOF and the rate of change of the EV cluster net output power to avoid short-term stability problems [9].

III. Frequency-Responsive EV charger stations

In this paper, the frequency response provided by EV charging stations is classified based on (a) Directionality of energy flow and (b) Flexibility of modifying the charging pattern.

(a) The directionality of energy flow. The EV charger stations can be either uni-directional or bi-directional. In the first case, the flow of energy is always from the power system to the vehicle, in this type of charger the only control available is the reduction of the charging power "smart charging" (V1G). In the second case, it is possible to discharge the battery of the EV to the power system and provide ancillary services; this operation is called "vehicle to the grid" (V2G).

(b) The flexibility of modifying the charging pattern. This property is closely related to the location of the charging facility.

(b.1) Private charging. EVs in this category are connected to the power system for longer durations, usually overnight [10] and the connection power is usually lower than 22 kW because of electrical system limitations. Most households in GB are supplied by single phase and with the main income fuse rated at between 60 to 80 A [11]. Given that the user knows in advance its desired state of charge (SOC) as well as the time at which the vehicle will be used, the control system of the charger can regulate the charging power of the battery. To charge an average 40 kWh battery takes between 4 to 6 hours using an 11 kW and a 7-kW charger respectively. If the connection time is longer than this, the vehicle can be charged at a percentage of its rated power (see Table I), enabling the

possibility of providing frequency response for over frequency events (see Fig 3).

(b.2) Public charging. The frequency response of this kind of EV charger represents the public charging stations with charging power greater than 22 kW. The reason for the high power of the station is to charge the EV as fast as possible; therefore in pre-fault conditions, the charging power is always the maximum that the station can provide and that is allowed by the EV. Vehicles connected at these stations do not have the possibility of providing frequency response for over frequency events (see Fig. 3).

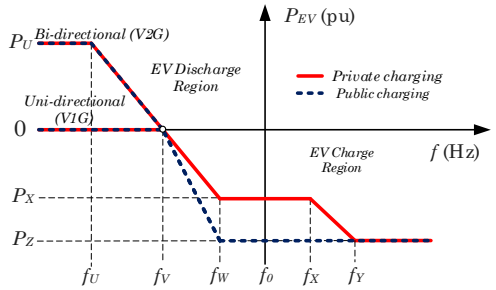

Fig. 3. Charging profile for EVs charging in a private charging station.

(b.3) Unresponsive. The EVs charger pattern constitutes a stiff load and does not provide intentional frequency support. The charger will disconnect automatically for frequencies lower than 47 Hz or higher than 52 Hz. They can be either charging or idle, depending on their SOC.

IV. EV Charging Demand

According to a high EV uptake scenario, there could be as much as 8 million EVs in GB by the year 2025 [3]. The impact that these EVs have on the SFR depends, among other factors, on the amount of EVs being charged at one specific time period and on the power consumption of the chargers.

A. Estimation of the EV demand

The EVs are classified according to their type [12] and according to the use of transport [13]. A charging profile for each vehicle is created by random sampling based on probability distributions for the battery capacity, daily travel range, maximum travel range and initial SOC. Charging station data is obtained from [14]. The individual EV daily demand profiles are aggregated to derive the total charging load for each different charging pattern.

B. Charging patterns

Various charging patterns are discussed in the literature in terms of the time at which the EV begins to charge [15], [16]. Three charging patterns are considered: (i) *Uncontrolled or "Dumb" charging*: The EV is plugged as soon as it is back from its daily trip and begins to charge immediately. It is modelled by a normal distribution with a mean value of 18:00 and a standard deviation of 4 hours [16]. (ii) *Dual tariff or "Off-peak" charging:* The EV user is incentivized to charge the EV within a specified time range corresponding to low system demand. The time of charging is uniformly distributed between 21:00 and 23:00 [16]. (iii) *Intelligent or "Smart":* The EV is plugged as soon as it is back from its daily trip, but a control system ensures that charging takes place when the electricity cost is the lowest (during system demand valley hours) [17].

Different EV daily demand scenarios are determined based on the proportion of EV owners aligned with the different charging patterns, and they are presented in Table II. The projected daily demand of the EVs in GB for the year 2025 is shown in Fig. 4.

TABLE I. PARAMETERS FOR *P-F* CHARACTERISTIC OF DIFFERENT CHARGING TYPES

Parameter	Private charging	Public charging	Unresponsive
P_U	V2G =1.00 pu V1G =0.00 pu	V2G =1.00 pu V1G =0.00 pu	N/A
P_X	-0.60 pu	N/A	-1.00 pu
P_Z	-1.00 pu	-1.00 pu	N/A
f_u	49.5 Hz	49.5 Hz	N/A
f_v	49.75 Hz	49.75 Hz	47 Hz
f_w	49.95 Hz	49.95 Hz	N/A
f_0	50 Hz	50 Hz	50 Hz
f_x	50.05 Hz	N/A	N/A
f_y	50.25 Hz	N/A	52 Hz

TABLE II. SCENARIOS FOR THE CHARGING TIME OF THE EV

Charging Scenario	(i) Dumb charging	(ii) Smart charging	(iii) off-peak charging
A_L	20 %	70 %	10 %
B_L	70 %	20 %	10 %
C_L	50 %	50 %	0 %

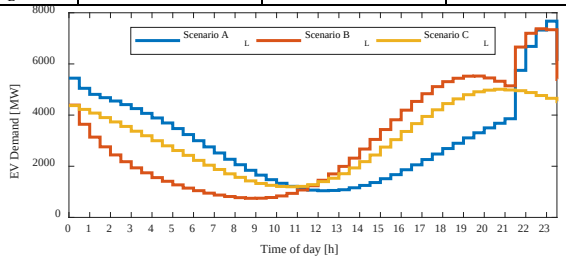

Fig. 4. Forecasted daily demand from EVs in GB for the year 2025.

In all scenarios, two demand peaks can be distinguished. The largest peak is related to the vehicles attached to the Off-peak charging scheme. In scenarios, A_L and B_L, both with 10% of the vehicles involved in Off-peak charging, the maximum EV load occur at around 23:00 h (peak of 7,600 MW). The second peak depends on the charging scheme. In scenario A_L, this peak occurs during the valley hours of the power system, at around 00:00 h (5,400 MW) whereas in scenario B_L, it coincides with the peak demand in the power system, around 19:00 h (5500 MW).

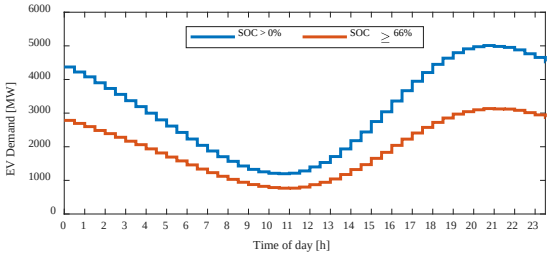

Fig. 5. EV demand for charging *Scenario* C_L, with *SOC*>0% and *SOC*≥66%.

Scenario C_L represents a smoother load profile with no *Off-peak charging* and the rest distributed evenly between *Dumb* and *Smart charging*. The maximum demand in this scenario occurs at around 20:30 h (5,000 MW). Since the main objective of EVs is to transport its users, it is reasonable to expect that only EVs with a SOC greater than a certain minimum value will allow their batteries to be depleted to provide frequency containment services. According to [18], most of the EV users charge their vehicles when the SOC is between 25 % to 66 %. Therefore, we have assumed that EVs with a SOC lower than 66 % are not involved in providing frequency containment services because their owners perceive the SOC of the EV as low. This has the effect of reducing the power available for frequency response services, as can be seen from Fig. 5, which shows the reduced demand for scenario C_L.

V. Simulation Scenarios

Table III shows the simulation scenarios created for this paper. The system frequency disturbance (SFD) is a loss of a generation of 1,800 MW, corresponding to the infrequent infeed loss risk in the GB system [19].

TABLE III. Summary of the Simulation Scenarios

Simulation Scenario	Effect to assess	Types	Time of disturbance
A	Type of charging	Uni or Bidirectional	Minimum *H*
B	Time constant of charger	Min = 35 ms Max = 100 ms	
C	Measurement delay	Min = 0.1 s Max = 1.5 s	
D	Time of charging	See Table II	Throughout the day in 30 min. intervals
E	EV penetration	See Table II	

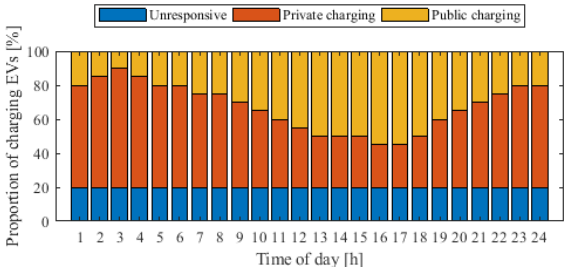

Fig. 6. Distribution of frequency response types.

For simulations scenarios A, B and C, the SFD is applied at the time of day corresponding to the minimum inertia, it allows obtaining the maximum frequency excursion. The minimum value of the system rotational inertia anticipated for the year 2025 is 70 GVA·s [3]. For scenarios D and E, the time of the disturbance is changed in a 30 minutes interval throughout the day, and the rotational inertia constant is also modified throughout the day according to the expected generation mix for the years of the study [3], [20]. The model used for the analysis is shown in Fig 1, with R = 4% [21] and D = 2.5% [22]. Typical values for TT = 300 ms, and Tg = 80 ms are used [16].

Depending on the time of day, the number of EVs connected to either *public* or *private charging stations* will change. The proportion has been estimated based on data from [10], [18] (Fig. 6). It reflects the fact EVs charging between 22:00 h and 07:00 h are more likely to be connected to private charging stations.

VI. Simulation Results & Discussion

A. Effect of the type of charging

Fig. 7 (a) shows the evolution of the system's frequency when the disturbance is applied at t = 1.0 s for the *Base Case* (without EV support) and for EV charging scenario A_L when the charging is both uni and bidirectional. The frequency response is improved in both cases with respect to the *Base Case*. The benefits of the bi-directional charging are a faster stabilization time as well as a smaller steady-state frequency deviation in steady-state.

TABLE IV. Simulation Cases With Different Types Of Charging

Simulation	EV charging scenario	Type of charging
Base Case	No EV frequency support	
Case A.1	*A*	Uni-directional
Case A.2	*A*	Bi-directional

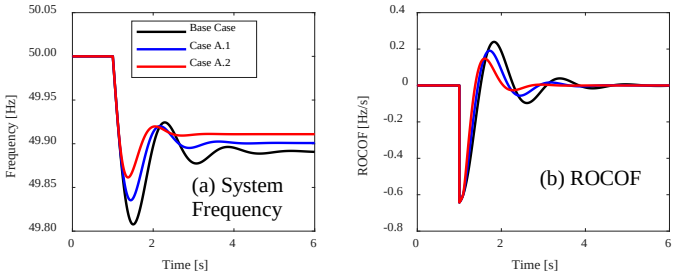

Fig. 7. Simulations results showing the effect of the type of charging.

The value of the $ROCOF_{max}$ remains constant because it depends only on the system's normalized inertia constant (H) and on the initial power imbalance (ΔP). As it is shown in Fig. 7 (b), the ROCOF has a quick stabilization time in the bidirectional case.

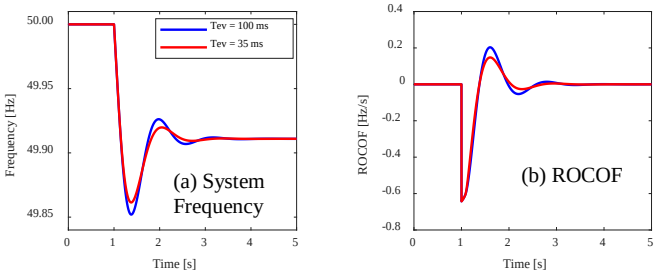

Fig. 8. Simulation results showing the effect of the EV charger time constant (T_{EV}).

B. Effect of the EV charger time constant

To observe the effect of the delay introduced by the EV charger, two simulations are performed with different values of the charger time constant T_{EV}. According to [10], [16] this value is in the range between T_{EV} = 35 ms and T_{EV} = 100 ms. The charging scenario corresponds to the *Case A.2* (Table IV). Fig. 8 shows that the minimum frequency value and the

stabilisation time are modified. The steady-state value of the frequency remains constant.

C. Effect of the measurement delay

Differences in infrastructure and technical specifications among charging stations will give rise to different measurement delays. To observe the effect of this on the frequency response provided by EVs, different combinations of measurement delays are assigned for *public* and *private charging stations*. The charging scenario considered corresponds to case *A.2* (Table IV), and Table V lists the different simulation cases.

TABLE V. SIMULATION SCENARIOS FOR THE MEASUREMENT DELAY

Simulation	Time of disturbance	Delay in public charging stations	Delay in private charging stations
Base Case	03:00 h	0.10 s	0.10 s
Case 1	03:00 h	1.50 s	0.10 s
Case 2	03:00 h	0.10 s	0.20 s
Case 3	03:00 h	0.10 s	0.25 s
Case 4	16:00 h	1.50 s	1.50 s

The frequency nadir decreases as the measurement delay increases (Fig. 9). It is found that the decrease in frequency nadir is not only proportional to the value of the delay inserted, but it is also highly sensitive to both the location of the delay and the time of the disturbance. If the delay is added to the charging station that is more loaded (and which, therefore, has more power available for frequency response), the effects on the frequency are greater.

In *Case 1*, a time delay of T_d = 1.5 s is added to the measurements of the public charging stations and the resulting frequency nadir decreased by 0.004 Hz compared to the Base Case. In *Case 2*, a delay of 0.2 s is added to the measurements of the *private charging stations* while the delay in the *public stations* are keep as per the Base Case, resulting in the frequency nadir decreasing by 0.01 Hz compared to the to the Base Case, In *Case 3*, the delay in the private charging stations is further increased to 0.25 s, leaving other delays as in the previous case. In *Case 4*, both delays are increased to 1.5 s, but the time of disturbance is changed to 16:00, corresponding to the time when the public charging stations are more loaded (Fig. 6), and when there is less overall EV demand in the scenario considered (Fig. 4). In this case, the frequency nadir decreased 0.01 Hz compared to *Case 3* but with less overshoot. See Fig. 10 (a) and Fig. 10 (b).

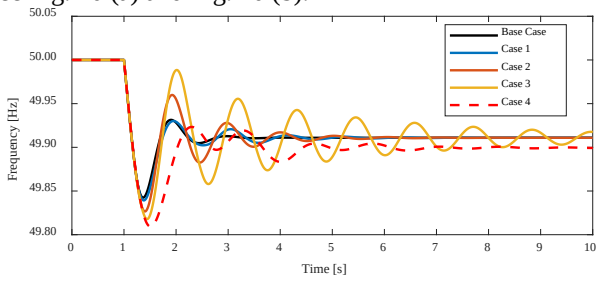

Fig. 9. Simulation results showing the effect of the measurement delay.

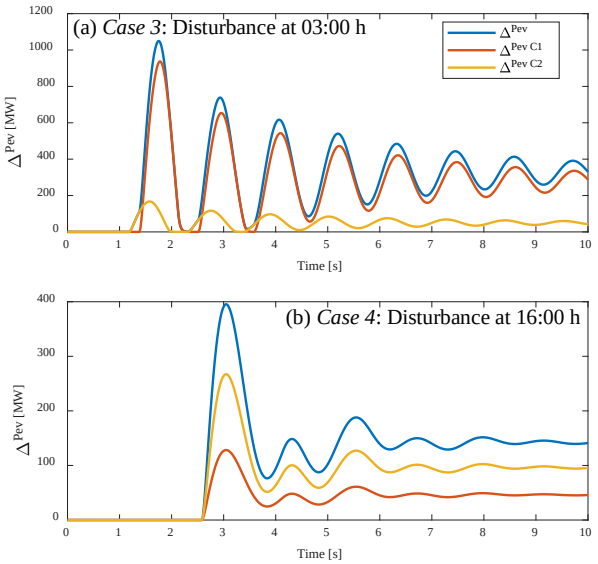

Fig. 10. Simulation results showing the effect of the measurement delay on ΔP_{EV}.

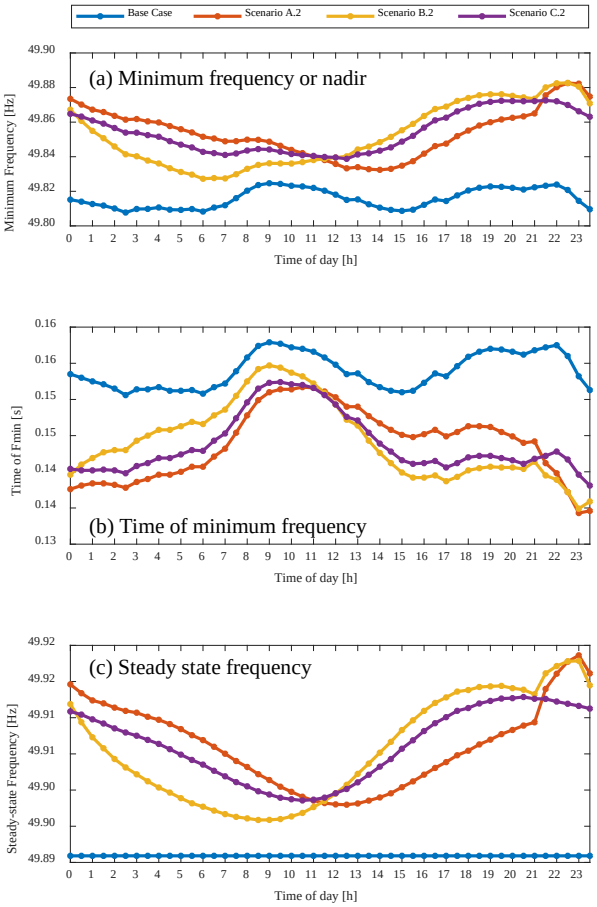

Fig. 11. Simulation results showing the effect of the time of charging: main SFR indicators.

D. Effect of the time of charging

The minimum frequency when the disturbance is applied at different times during the day is shown in Fig. 11 (a). In all the cases when EVs are providing frequency response, the frequency nadir of the system is higher. The time in which the frequency reaches its minimum value is plotted in Fig. 11 (b). The smaller this value is, the faster the frequency stops falling and starts increasing. For all scenarios with EVs, this value is smaller than the *Base Case*. Fig. 11 (c) depicts the steady-state frequency. As shown in section VI.A, this value does not depend on the system's inertia. Therefore, it remains constant in the base case when the disturbance is applied at different times during the day.

E. Effect of the EV penetration

Different estimations for the number of EVs on the road by the year 2025 are obtained from [3]. The Base Case is without support from EVs whereas *Case 1* corresponds to a high EV uptake, *Case 2* to the "Two Degrees" scenario and *Case 3* to the "Steady State" scenario. Charging scenario C_L of Table II with bi-directional charging and minimum delays are considered. In all cases, the frequency nadir is higher (less frequency deviation) when EVs provide frequency support. As the number of EVs increases, the frequency nadir increases (Fig. 12). However, the ROCOF value remains constant.

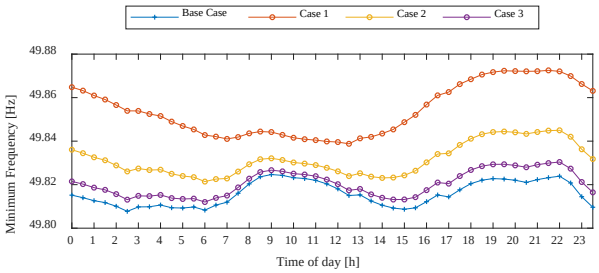

Fig. 12. Simulation results showing the effect of EV penetration on the frequency nadir.

VII. Conclusions and Future Work

The improvement of the frequency response following a disturbance has been observed when a vast number of EVs are connected to charging stations equipped to provide unidirectional or bidirectional charging, with superior results in the latter case. The delay introduced by the EV charging apparatus does not result in a deterioration of the frequency response. However the delay introduced by the measurement equipment has a significant impact on the dynamics observed. With the growth in the number of charging stations equipped to provide bi-directional charging, the potential for the provision of fast active power injection during frequency excursions is expanding rapidly. But, as more power is handled by the charging stations, the chance that poorly set controllers or long delays in measurement produce negative effects on the system's frequency by overcompensating increases. Future work will focus on the effect of using different dead bands as well as different slopes in the power-frequency characteristic of the EV cluster. Additionally, a more detailed model of the power system will be used to consider the geographic location of the chargers and the effect this has on the frequency services provided.

References

[1] International Energy Agency, "Global EV Outlook 2017 Together Secure Sustainable Global EV outlook 2017."

[2] D. Wang, J. Coignard, T. Zeng, C. Zhang, and S. Saxena, "Quantifying electric vehicle battery degradation from driving vs vehicle-to-grid services," *J. Power Sources*, vol. 332, 2016.

[3] National Grid, "Future Energy Scenarios," 2017.

[4] J. García-Villalobos, I. Zamora, J. I. San Martín, F. J. Asensio, and V. Aperribay, "Plug-in electric vehicles in electric distribution networks: A review of smart charging approaches," *Renew. Sustain. Energy Rev.*, vol. 38, pp. 717–731, 2014.

[5] V. T. Sæmundsson, M. Rezkalla, A. Zecchino, and M. Marinelli, "Aggregation of Single-phase Electric Vehicles for Frequency Control Provision Based on Unidirectional Charging," *52nd Int. Univ. Power Eng. Conf.*, pp. 1–6, 2017.

[6] S. Izadkhast, P. Garcia-Gonzalez, P. Frias, and P. Bauer, "Design of Plug-in Electric Vehicle's Frequency-Droop Controller for Primary Frequency Control and Performance Assessment," *IEEE Trans. Power Syst.*, vol. 32, no. 6, pp. 1–1, 2017.

[7] J. Meng *et al.*, "Dynamic frequency response from electric vehicles considering travelling behaviour in the Great Britain power system," *Appl. Energy*, vol. 162, pp. 966–979, Jan. 2016.

[8] H. Bevrani, "Robust Power System Frequency Control," in *Chapter 2*, 2014.

[9] D. M. Greenwood, K. Y. Lim, C. Patsios, P. F. Lyons, Y. S. Lim, and P. C. Taylor, "Frequency response services designed for energy storage," *Appl. Energy*, vol. 203, pp. 115–127, 2017.

[10] J. Meng, Y. Mu, J. Wu, H. Jia, Q. Dai, and X. Yu, "Dynamic frequency response from electric vehicles in the Great Britain power system."

[11] National Grid, "Mass fast charging of electric vehicles," 2017. [Online]. Available: http://fes.nationalgrid.com/media/1281/forecourt-thoughts-v12.pdf. [Accessed: 16-Feb-2018].

[12] "Vehicle categories - European Commission." [Online]. Available: https://ec.europa.eu/transport/road_safety/topics/vehicles/vehicle_categories_en. [Accessed: 02-Jan-2018].

[13] R. Ball, N. Keers, M. Alexander, and E. Bower, "MERGE Project - D2.1 - Modelling electric storage devices for EV," no. January, pp. 1–135, 2010.

[14] "Open Charge Map." [Online]. Available: https://www.openchargemap.org/site/. [Accessed: 31-Jan-2018].

[15] R. J. Bessa and M. A. Matos, "Economic and technical management of an aggregation agent for electric vehicles: A literature survey," *Eur. Trans. Electr. Power*, vol. 22, no. 3, pp. 334–350, 2012.

[16] Y. Mu, J. Wu, J. Ekanayake, N. Jenkins, and H. Jia, "Primary Frequency Response From Electric Vehicles in the Great Britain Power System," *Smart Grid, IEEE Trans.*, vol. 4, no. 2, pp. 1142–1150, Jun. 2013.

[17] K. Qian, C. Zhou, M. Allan, and Y. Yuan, "Modeling of load demand due to EV battery charging in distribution systems," *IEEE Trans. Power Syst.*, vol. 26, no. 2, pp. 802–810, 2011.

[18] EA Technology and Manchester University, "An Assesment of how much headroom an Esprit type technology would yield," 2015.

[19] National Grid, "National Electricity Transmission System Security and Quality of Supply Standard," vol. Ver. 2.3, no. March, p. 59, 2017.

[20] National Grid, "Electricity Ten Year Statement 2017," *UK electricity transmission*, 2017. [Online]. Available: http://www2.nationalgrid.com/UK/Industry-information/Future-of-Energy/Electricity-Ten-Year-Statement/%5Cnhttp://www2.nationalgrid.com/WorkArea/DownloadAsset.aspx?id=44084. [Accessed: 16-Feb-2018].

[21] National Grid, E. Transmission, E. Act, G. Britain, and P. Act, "The grid code," no. 5, 2015.

[22] National Grid, "System Operability Framework 2016," 2016.